

EVS24
Stavanger, Norway, May 13-16, 2009

Modeling and Simulation of an Autonomous Hybrid-Electric Military Vehicle

David Milner¹, Jarrett Goodell², Wilford Smith³, Mike Pozolo⁴, Jason Ueda⁵

¹*SAIC Inc, 4901 Olde Towne Parkway Suite 200 Marietta GA 30068 USA, milnerd@saic.com*

²*SAIC Inc, 8303 North Mopac Expressway Suite B-450 Austin, TX 78759 USA, goodellja@saic.com*

³*SAIC Inc, 4901 Olde Towne Parkway Suite 200 Marietta GA 30068 USA, smithw@saic.com*

⁴*U.S. Army RDECOM-TARDEC, MS 159 US Army Tank Automotive Command AMSRD-TAR-R 6501 E 11 Mile Road Warren, MI 483970001 USA, mike.pozolo@us.army.mil*

⁵*U.S. Army RDECOM-TARDEC, MS 159 US Army Tank Automotive Command AMSRD-TAR-R 6501 E 11 Mile Road Warren, MI 483970001 USA, jason.ueda@us.army.mil*

Abstract

The U.S. Army TACOM-TARDEC developed and validated a high-fidelity six-degree-of-freedom model to use in a trade study for the development of a prototype autonomous vehicle. The model captures realistic dynamics of the six-wheeled, skid-steered vehicle along with the electrical, thermal, and mechanical response of a detailed series hybrid-electric power system with in-hub drive motors, lithium-ion battery, and generator linked to a diesel engine. These components were modeled and integrated via extensive power and energy component libraries developed for use with a high-fidelity software tool for dynamics modeling. Further, the vehicle model's entire complement of components was integrated in a flexible configuration that allowed them to be readily adjusted or swapped out so the user could use the model to ascertain the relative effects of modifying the vehicle's structural or power system components on specific vehicle evaluation criteria. Such criteria include the vehicle's performance with high-speed stability, skid steering stability, body pitch/roll/dive/squat characteristics, braking capability, road/soft-soil traversal, and steering maneuverability.

The model captures both the on- and off-road mobility for the vehicle via use of an extensive library of various terrains including hard surface, sand, sandy loam, clay soil, and snow. Further, detailed waypoint-based path navigation routines automate the vehicle's traversal over a number of user-selectable courses including some established military courses such as Churchville-B, Perryman 1, 3, and A, and Munson with user-defined vehicle velocities. The model functions as an executable file run independent of any proprietary or close-source software; the user utilizes a simplified interface to vary any of the variables associated with the vehicle's geometry, power system, course and speed to navigate, and terrain type applied to the course. The graphical view for the vehicle traversing the selected terrain is shown with an open source 3D graphics tool. The model was validated by applying the specifications in the model for the

prototype vehicle of the first-generation of autonomous six-wheeled skid-steered vehicle, simulating the model in maneuvers identical to those the prototype vehicle performed, and comparing the simulated and actual results; the data matched and the model was successfully validated.

The vehicle model was designed primarily for the trade study for the design of a specific vehicle, but was created with sufficient flexibility and capability for modeling future vehicles as well. The interchangeability of the vehicle models' components and environments allow a user to modify or replace the vehicle's power system components, chassis masses, tires, transmission, duty cycles, courses to traverse, and many other aspects of the vehicle. Thus the user can essentially model any vehicle with similar types of components or structures and use that model to determine the impact of those elements upon many vehicle design considerations such as mass requirements, volume constraints, power system requirements, wheels design, suspension characteristics, and controls. Several new vehicle models are already being developed using this model's flexibility and capability.

Keywords: HEV (hybrid electric vehicle), mobility, modeling, powertrain, regenerative braking

1 Introduction

The U.S. Army TACOM-TARDEC has modeled and validated a full six-degree-of-freedom six-wheeled hybrid-electric skid-steered vehicle with high-fidelity modeling software to be representative of its newly designed special operations vehicle. The model uses the modeling software's advanced suite of library components of physical actuators and system components that simulate realistic dynamics, power system layouts and controls, and an assortment of newly designed electrical, mechanical, and thermal components.

The advanced vehicle model was designed for use in comparing the relative effects of varying the vehicle's structural layout and power system design upon the vehicle's mobility performance. Specific performance criteria included the vehicle's acceleration, high-speed stability, skid steering stability, body pitch/roll/dive/squat handling, high-speed braking, and traversal and steering over both on- and off-road soil conditions.

All of the vehicle's components and simulated environmental conditions are easily and quickly interchangeable or alterable for this purpose. This includes the vehicle's engine, gears, motors, battery, distribution of mass, tires, hub gearing, and/or traction motors with respect to vehicle design considerations such as mass, volume, regenerative braking system, hybrid power

system, wheels, suspension, and controls. This continues the work described in Milner [2].

2 Vehicle Model

The vehicle model was constructed with fully integrated vehicle component systems including the 6-DOF vehicle chassis, six independently driven wheels with pneumatic (compressible) tires, roadarm suspension systems with bump-limits and independent orientations for each wheel, in-hub wheel motors linked to a series hybrid-electric power train complete with a diesel engine and lithium-ion battery, autonomous navigation algorithms for path navigation, power system management controls, detailed terrain packages with surface geometries, variables and functions for both on-road and off-road (soft-soil) terrains, terrain-to-wheel force and moment calculations, and environmental effects such as gravitational and air drag forces.

The vehicle simulation calculates all pertinent forces and moments on the vehicle. These forces include those from soil and wheel deformation, lateral and longitudinal wheel slip, traction and normal terrain-wheel forces, suspension forces and deflections, power system loads, 6-DOF chassis motion, etc. The model also accounts for all force and motion interactions between the wheels, the suspension linkages attached to each respective wheel, and the chassis attached to each wheel's suspension.

The model was validated with data for comparable vehicles, and can be run as a standalone executable. Fig.1 shows the top level of the vehicle model with representations for the complete vehicle structure, hybrid-electric power systems, and path navigation control systems. Fig.2 shows a sample 3-D graphical rendering of the vehicle model.

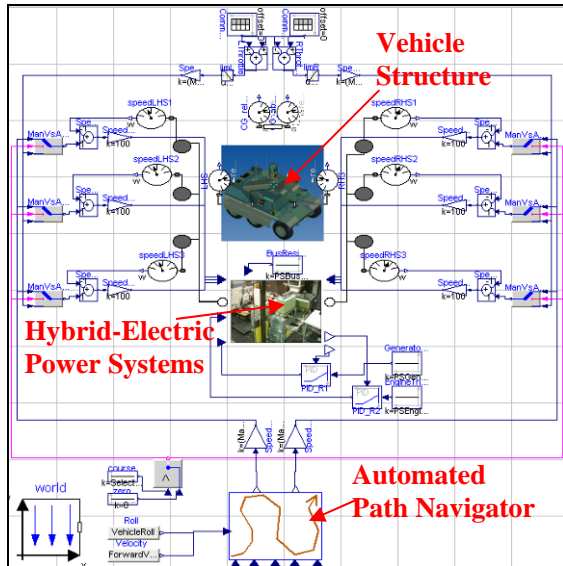


Figure1: Top-Level View of Vehicle Model



Figure2: Graphical Rendering of Vehicle (bottom)

2.1 Vehicle Structure

The vehicle structure in the model consists of integrated subsystems for the vehicle chassis, six independent wheels, and bump-limited roadarm suspension systems for each wheel as shown in Fig.3. The vehicle body (chassis) is the green vehicle central in the figure, and

incorporates variables for all the vehicle's sprung and un-sprung masses, dimensions, moments of inertia, and center of gravity.

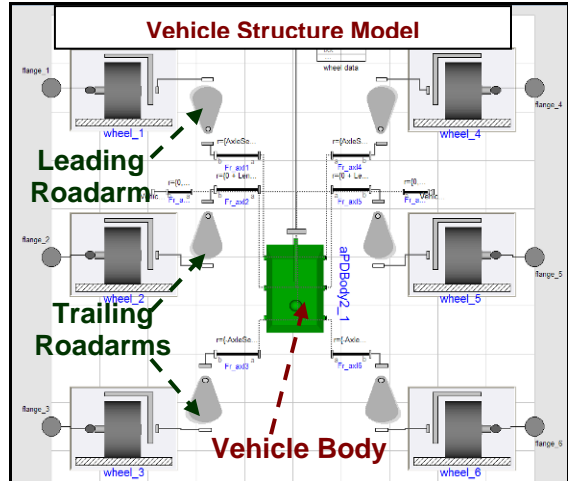


Figure3: Vehicle Model with 6 Wheels, and Leading-Trailing-Roadarm Configuration

The roadarms are each connected to both one wheel and one unique attachment point on the vehicle's chassis. They are oriented in a leading-trailing-trailing configuration for the front, middle, and rear wheels respectively on both sides of the vehicle as shown in the picture. The vehicle structure model effectively captures the resultant vehicle movements of the vehicle's components due to all forces working on the vehicle's wheels and propagated through the vehicle's wheels and suspension system to the chassis; such forces include drive forces from the power system, and resistive forces from gravity, air drag, and the wheel-terrain interactions.

2.2 Roadarm Suspension

The suspension system is comprised of six roadarms connecting the vehicle chassis to the hub of each wheel. The roadarms are rigid masses that connect the vehicle body to the wheels as the primary suspension system as shown in Fig.4. They include a strut spring-damper system with specified spring, damping, and un-stretched length, and specific points of attachment to both the chassis and roadarm. This is a passive suspension system designed for optimizing weight and space savings on the vehicle. The maximum vertical displacement of the roadarm is limited by bump limiters.

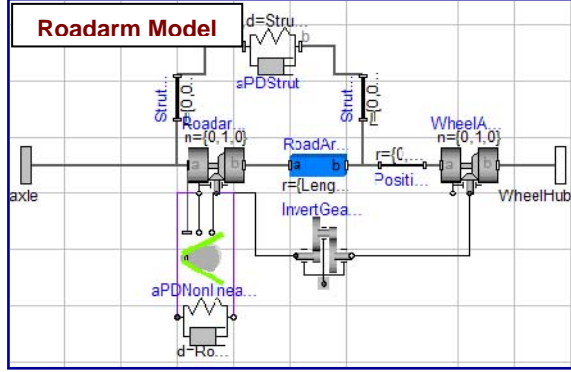


Figure4: Roadarm Suspension Configuration for Wheels

The roadarms are connected at one end directly to the vehicle chassis at points denoted as “roadarm attachment points”, and at its other end to the hub of one wheel. These points are shown on the wheel picture in Fig.5.

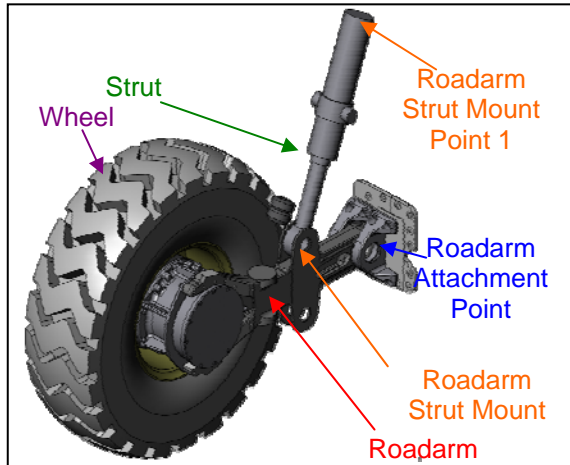


Figure5: Roadarm Suspension Configuration for Wheels

2.3 Wheels

The wheels of the vehicle model are an empirically derived design that encompass both on-road and off-road mobility calculations for the vehicle model. The wheel model includes a compressible pneumatic tire mass with a primary rotational degree of freedom about its hub mass that is affixed to the hub end of the roadarm.

The traction motors mounted within each wheel hub provide torque directly to the wheel's rotating tire through the power system's final drive. The wheel model calculates the resultant forces acting upon the wheel based on empirical formulations of both on-road (paved surfaces) and off-road (soft soil) terrain-wheel force calculations; the on-road forces were based upon the interpolated force-slip curves for normal tire

loads, and the off-road forces were based upon off-road terrain-tire force calculations presented in Wong [4], with simplifications based upon equations from Shibly [3]. The model performs all transformation calculations included for all forces & coordinate frames of the wheel's connection points. The resultant forces are propagated through the roadarms to the integrated vehicle model.

The wheel was specified based upon a right-hand XYZ coordinate system located at the center of the wheel P_c , with axis X_c oriented in the forward direction of the wheel, axis Y_c oriented to the left of the forward direction and perpendicular to X_c , and Z_c oriented up as shown in Fig.6. The wheel's tire geometry was defined with un-deformed radius R , width w , and deformed tire deflection Δz . The contact patch of the wheel was defined with length L_{cp} , width w (same as wheel width), and equivalent contact point P_i . An equivalent point of contact was defined for the point where equivalent forces F_x , F_y , and F_z , and moments M_x , M_y , and M_z are representative of all the ground loads acting the contact patch of the tire. The contact point is located displaced from the exact bottom-center point of the wheel by dL_x and dL_y in the X (longitudinal) and Y (lateral) directions respectively.

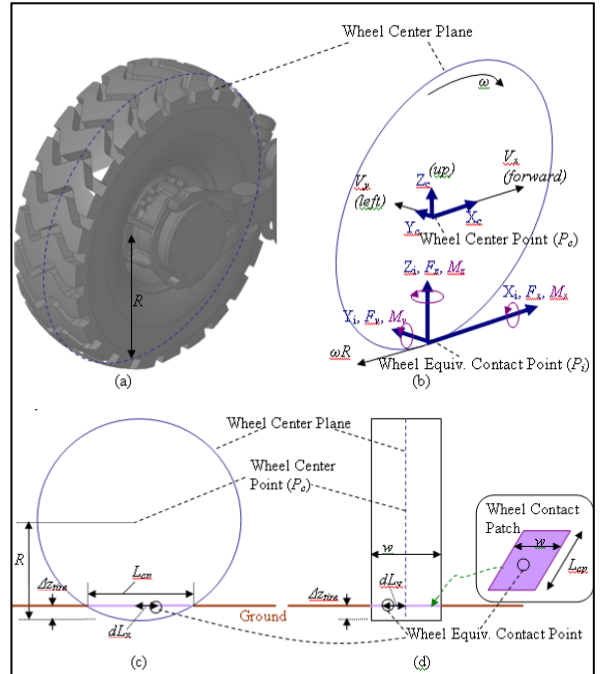


Figure6: Wheel Description including (a) Isometric View, (b) Isometric Drawing Coordinate Axes and Sign Convention (c) Side View with Dimensions, and (d) Front View and Contact Patch

The forces acting upon the contact point for on-road conditions were calculated based upon both the deflection of the equivalent terrain-wheel contact point, the stiffness/damping characteristics of the tire surface, and empirically derived force-slip curves based on nominal (expected) loads for typical truck tires. The longitudinal and lateral terrain-wheel forces were calculated uniquely for each wheel by interpolating between two representative force-slip curves for these tires for the normal load on the wheel and the instantaneous *Slip* of the tire. The force-slip curves were defined in the model based upon a curve-fit for specific features of the curves including zero slip, slip of the maximum tire force, maximum longitudinal tire force, slip at sliding, and tire force at sliding as indicated in Fig.7. The *Slip* is the negative difference between the speed of the center of the wheel (V) and the speed of the wheel at the point of contact with the road all divided by the speed of the wheel, or wheel rotational speed multiplied by the wheel radius ($\omega \cdot R$).

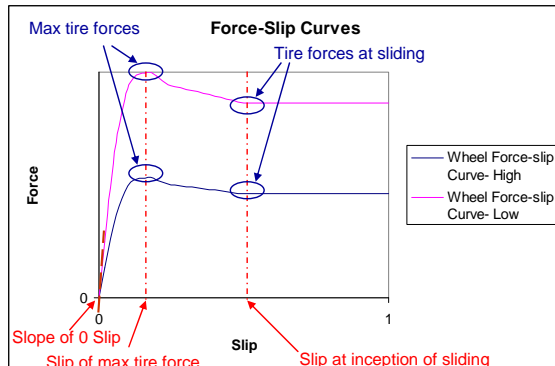


Figure 7: Force-Slip Curves Used for Calculating On-Road Tire Forces

The terrain-wheel forces for off-road vehicle traversal included resistive forces from soft-soil terrain-to-wheel interactions. These primary soft-soil resistive forces included longitudinal and lateral off-road forces and off-road moment due to soil compression, shear, and bulldozing forces. These off-road forces and moment were calculated based upon the approximation of the pressure distribution acting upon the tire due to the sinkage of the wheel into the ground.

Shibly [3] defined the normal pressure and shear force approximation acting upon the tire with respect to the sinkage of the tire into the terrain. This calculation is applied in the model to determine along with the characteristics of the off-road terrain as described in Wong [4] for

various types of soil. All details for the terrain forces are provided in Milner [2].

2.4 Path Navigator

The automated path navigation system simulates driver inputs suitable for automated driving course negotiation. The path navigator uses a waypoint-based navigation algorithm that tracks the vehicle's position with respect to a predetermined course described by waypoints that define the desired trajectory for the vehicle to follow. This tracks and actively minimizes the vehicle's body-fixed lateral and heading errors with respect to the desired path by providing either direct torque commands to the left and right side motors of the power system to successfully navigate a course. This is described further in Compere [1].

The path navigator outputs torque commands to the left/right motors for this skid-steered vehicle. The model maintains smooth and stable steering inputs by using look-ahead functions to apply torque commands/steer angles to minimize heading error and lateral error indicated in Fig.8.

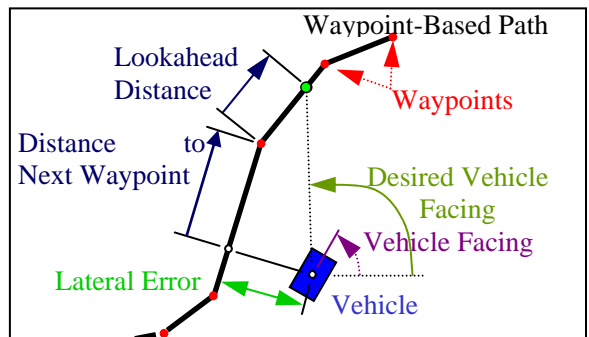


Figure 8: Path Navigator's Discretized Waypoint-Based Path Approximating the Desired Path to Follow

The model is loaded with six courses: Churchville B, Perryman A, Perryman 3, Perryman 1-Outer, a Combination Churchville/ Perryman/ Munson course, the full Munson course, and a Flat plane course. The Perryman courses are shown in Fig.9.

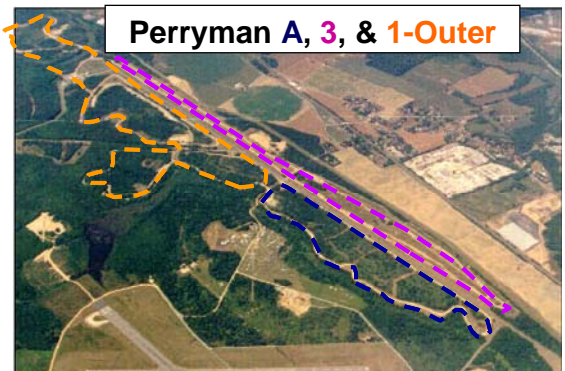


Figure9: Perryman A, 3, and 1-Outer Courses

2.5 Power System

The power system model is a series hybrid-electric power system. The model was assembled with components from both an electrical component library and custom-designed code. The power system includes six induction traction motors, with one located within each wheel hub. The motors are linked to a battery, engine, generator as part of an integrated “engine-generator-battery” power system set as shown in Fig.10.

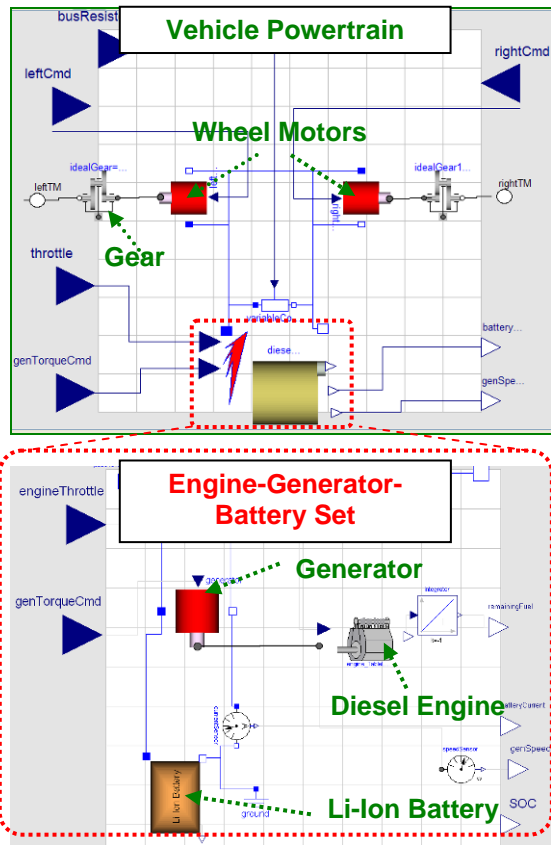


Figure10: Series Hybrid-Electric Power System Model and Components

The power system components are representative of actual components being designed for the vehicle. The battery is an equivalent circuit of a Lithium-Ion battery, and includes SOC and temperature-dependence functions for its resistors, capacitors, and voltage source parameters. The engine includes a torque-speed lookup table linked to an engine shaft and lookup table calculations for engine brake specific fuel consumption. The motors and generators include electromotive torques applied to rotational inertias that are linked to the final drives of each

wheel. The power system is controlled directly from path navigation control outputs.

2.6 Graphics

The graphics is an open source software suite utilized to provide the graphical output for the simulation in a non-proprietary executable version. The vehicle was visually rendered, then converted to a mesh, and inserted in a graphical rendering tool. The graphics tool shows the vehicle traversing the terrain based upon direct data inputs ported from the output of the executable simulation. The graphics script was setup with the rendered vehicle, and all three off-road courses loaded into the simulation. The vehicle is shown rendered with the Churchville B terrain in Fig.11.



Figure11: Graphic Rendering of Vehicle Model Traversing Terrain

3 Results

3.1 Model Validation

The vehicle model was validated to experimental skid-steer data obtained for a similarly designed prototype vehicle. The validation involved a 10 second, 360° skid turn of the vehicle. The simulated vehicle rolled into the skid turn as in Fig.12 with a $\sim 13.5^\circ$ roll angle which was comparable to the $\sim 14.5^\circ$ roll angle of the actual vehicle. The modeled and actual roadarms of the vehicle’s suspension system deflected to similar angles during the turn to achieve this vehicle roll.

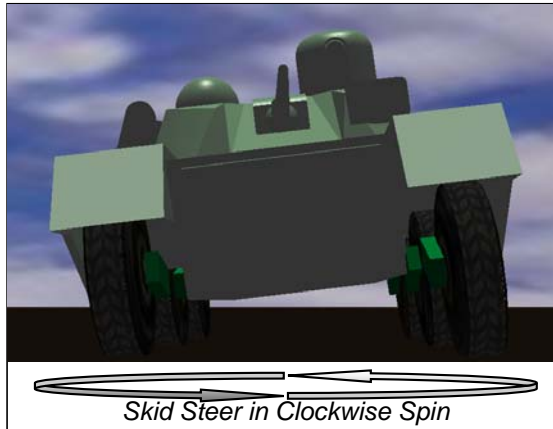


Figure12: Vehicle Rolling During Clockwise Skid-Steer

The motor speeds and torques matched well during the skid steer. The motor speed data vs. time aligned well for all motors for the modeled and actual vehicle skid steering data as shown in Table 1. Further, the total motor torque applied to each side of the vehicle aligned well between the actual and modeled data, but the motor torques for individual motors had significant differences for the front and rear motors.

Table1: Actual and Modeled Motor Torques for Vehicle Model Validation

Motor Group	Avg. Motor Torques (N-m)		Avg. Motor Speeds (rad/s)	
	Actual	Modeled	Actual	Modeled
Left motors	157	153	79	82
Right motors	165	157	-77	-82
Left front motor	29	87.0	80	84
Left middle motor	327	285	78	79
Left rear motor	116	88	80	83
Right front motor	75	128	-80	-83
Right middle motor	344	253	-70	-79
Right rear motor	78	92	-80	-84

The vehicle was verified to perform realistically for the skid-steer simulation. The vehicle rolled into the spin as is typical of skid-steered wheeled vehicles with the leading/trailing/trailing roadarm suspension configuration. The overall motor and wheel speed characteristics matched well with the actual data. There were minor discrepancies on motoring loads for individual wheels when compared to the actual data, but these were attributable to the actual vehicle's chassis lacking perfect rigidity and thus distributing the load more evenly among its tires.

3.2 Simulation Results

The model was primarily used as a tool for determining the high-speed stability performance of the vehicle with the components and power system determined in the trade study. The vehicle was simulated in a high-speed figure-S lane change maneuver to show it performed on-road. The vehicle was essentially simulated at a forward velocity of 25 m/s when it made a ~2 meter lane change and then resumed driving straight all while maintaining its speed. Fig.13 shows the animation output from a simulation of the vehicle performing a lane-change S-pattern maneuver at high speed.

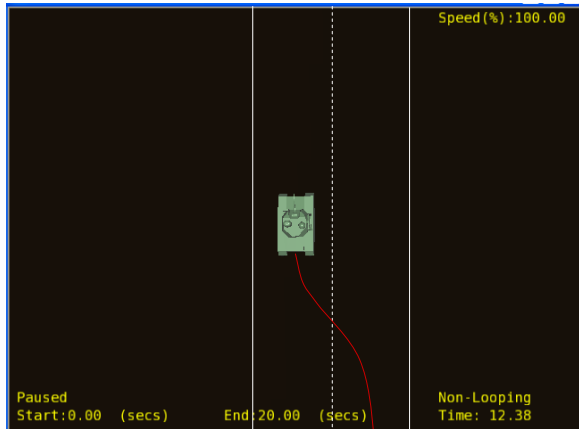


Figure13: Vehicle Performing a High-Speed Lane-Change Maneuver

The vehicle performed the maneuver well without rolling excessively ($<8.25^\circ$) and resumed its path one lane over. The power system drew significant power up to 150kW from the generator/battery for the initial acceleration, but then required minimal power to conduct the maneuver (<10 kW from the engine, and 15kW from the generator) for the majority of the high-speed simulation. This was partly supplemented from the regenerative capacity of the inner wheel motors. The Fig.14 shows time-based data of the vehicle's dynamic

status and overall power system draws from the engine and generator during the turn.

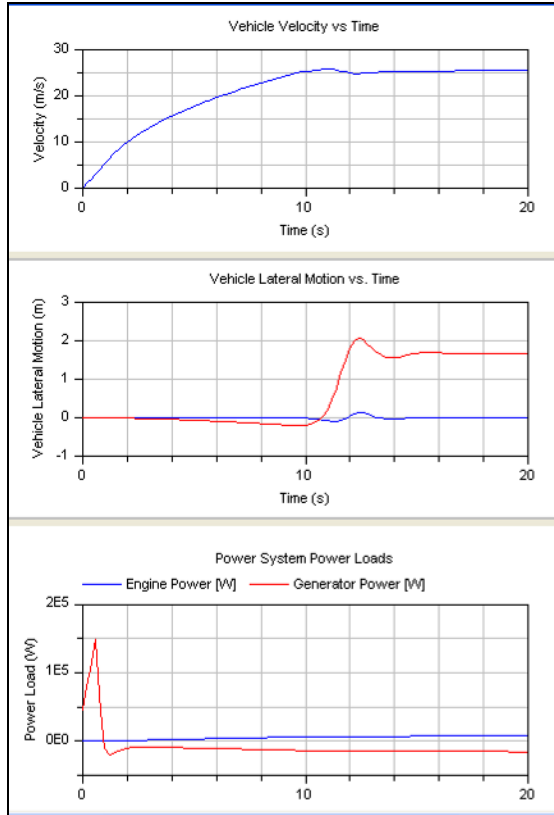


Figure 14: Vehicle's Dynamic Status and Power System Draws during the Turn

4 Conclusions

The model for the advanced unmanned prototype vehicle was completed and verified to be an accurate representation of a full 6-DOF 6-wheeled skid-steered series hybrid-electric vehicle. The model was developed with extensive capabilities for evaluating both on-road and off-road vehicle performance while allowing the user to modify the components and simulation setup as desired. The model enables the user to assign any desired modifications to virtually all of the major vehicle and simulation parameters such as vehicle dimensions, masses, rotational inertias, center of gravity, roadarm/strut characteristics, wheel characteristics, engine and motor performance characteristics, course selection, terrain surface type, etc to determine the relative impacts of such changes upon the vehicle's performance. The model was validated against actual vehicle mobility data from a comparable prototype vehicle. The performance of the vehicle has been verified to be a useful and accurate

comparative tool for this vehicle type. Therefore, it is an advantageous tool for the government for the design and simulation of a wide variety of component layouts and simulated conditions for modern unmanned or manned prototype skid-steered ground vehicles. It could provide the basis for many future vehicle modeling endeavors.

References

- [1] Compere, M., Tracked Vehicle Mobility Modeling and Simulation, September 2007
- [2] Milner, D, Goodel J., Smith W., Pozolo, M., Ueda, J.; Modeling of an Unmanned Six-Wheeled Skid-Steered Hybrid-Electric Military Vehicle, U.S Army RDECOM TARDEC., November 18, 2008.
- [3] Shibly H., Iagnemma K., Dubowsky, S., An Equivalent Soil Mechanics Formulation for Rigid Wheels in Deformable Terrain, With Application to Planetary Exploration Rovers, Journal of Terramechanics 42 (2005) 1-13. Cambridge MA, July 2004
- [4] Wong, Theory of Ground Vehicles, 3rd ed., John Wiley & Sons, NY, 2001

Authors

DAVID MILNER is a mechanical engineer with SAIC working with the US Army TACOM's P&E-SIL developing hybrid power systems modeling and simulation tools. His research interests include modeling of integrated military vehicle dynamics, controls, mobility and power systems. He holds a MS in Mechanical Engineering from the Georgian Institute of Technology, a BS in Mechanical Engineering from the University of Florida, and a Minor in Materials and Science Engineering from the University of Florida.

JARRETT GOODELL is a mechanical engineering analyst with SAIC working with the US Army TACOM's P&E-SIL developing hybrid power systems modeling and simulation tools. His interests include vehicle dynamics, control systems, and distributed real time modeling and simulation. He holds a MS in Mechanical Engineering from The University of Texas at Austin and a BS in Mechanical Engineering from Purdue University.

WILFORD SMITH is a Principal Scientist with SAIC working with the US Army TACOM's P&E-SIL developing hybrid power systems modeling and simulation tools. His research interests include multi-resolution modeling of power systems and distributed real time modeling and simulation. He holds a MS in Mechanical Engineering from the University of Michigan and a BS in Mechanical Engineering from the Georgia Institute of Technology.

MIKE POZOLO is a senior engineer with the U.S. Army RDECOM-TARDEC Ground Vehicle Power and Mobility Group. He is the Team Leader for

Powertrain Modeling and Simulation. His interests include advanced propulsion systems for military applications and drive cycle development for evaluation of advanced propulsion systems. He holds a B.S. in Mechanical Engineering from Wayne State University as well as an M.B.A. from Western Michigan University

JASON UEDA is an engineer with the U.S. Army RDECOM-TARDEC Ground Vehicle Power and Mobility Group. He is a member of the Powertrain Modeling and Simulation group.